

HyperGLM: HyperGraph for Video Scene Graph Generation and Anticipation

Trong-Thuan Nguyen^{1†}, Pha Nguyen^{1†}, Jackson Cothren¹, Alper Yilmaz², Khoa Luu¹

¹University of Arkansas ²Ohio State University

¹{thuann, panguyen, jcorthre, khoaluu}@uark.edu ²yilmaz.15@osu.edu

uark-cviu.github.io/projects/HyperGLM

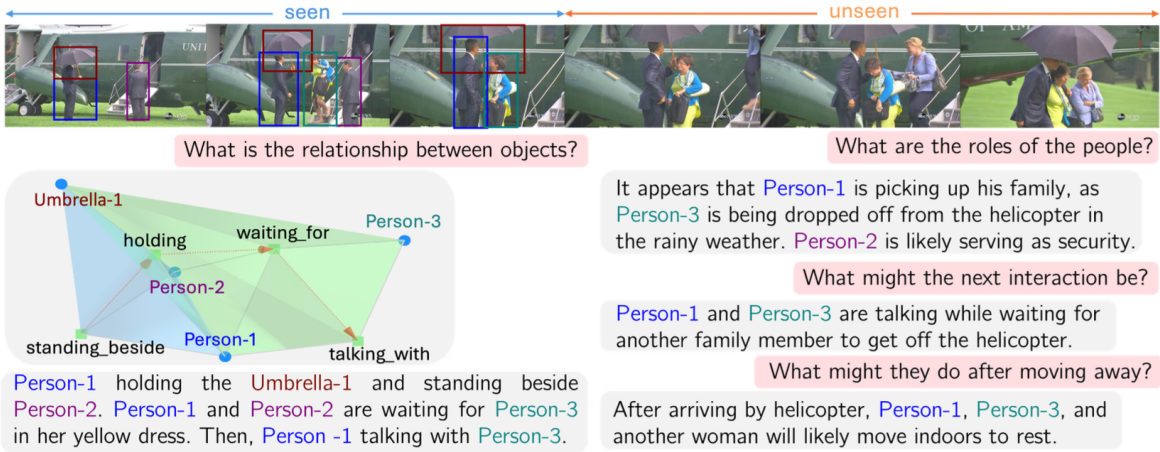


Figure 1. Our HyperGLM framework supports Video Scene Graph Generation, Anticipation, and Reasoning. HyperGLM constructs scene graphs from observed video frames and predicts relationships in unseen frames by leveraging a unified hypergraph for temporal modeling and comprehensive understanding.

Abstract

Multimodal LLMs have advanced vision-language tasks but still struggle with understanding video scenes. To bridge this gap, Video Scene Graph Generation (VidSGG) has emerged to capture multi-object relationships across video frames. However, prior methods rely on pairwise connections, limiting their ability to handle complex multi-object interactions and reasoning. To this end, we propose the Multimodal Large Language Models (LLMs) on a Scene HyperGraph (HyperGLM), promoting reasoning about multi-way interactions and higher-order relationships. Our approach uniquely integrates entity scene graphs, which capture spatial relationships between objects, with a procedural graph that models their causal transitions, forming a unified HyperGraph. Significantly, HyperGLM enables reasoning by injecting this unified HyperGraph into LLMs. Additionally, we introduce a new Video Scene Graph Reasoning (VSGR) dataset featuring 1.9M frames from third-person, egocentric, and drone views and support five tasks. Empirically, HyperGLM consistently outperforms state-of-the-art methods, effectively modeling and reasoning complex relationships in diverse scenes.

† Equal contribution.

1. Introduction

In recent years, Multimodal Large Language Models (LLMs) [2, 10] have set new benchmarks, with vision-language models excelling in diverse multimodal tasks. However, fully understanding dynamic video scenes remains a significant challenge for applications like autonomous driving, intelligent surveillance, human-object interaction, and multimedia analysis. Towards this goal, Video Scene Graph Generation (VidSGG) [18, 52] has emerged as a critical task for capturing multi-object relationships across video frames. In particular, VidSGG enables high-level tasks such as event forecasting [36, 43, 45], video captioning [24, 38, 40], and video question answering [20, 30, 32, 41] by constructing detailed representations of entities and their interactions.

However, prior VidSGG methods and datasets have limited capacity for comprehensive video understanding. Traditional scene graph-based methods [4, 34, 35, 42] only model pairwise object relationships within single frames, making it challenging to capture higher-order relationships and temporal dependencies in real-world scenarios. Additionally, existing benchmark datasets [18, 34, 35, 52] focus is primarily confined to Scene Graph Generation (SGG) and Scene

Graph Anticipation (SGA) tasks, lacking annotations for reasoning tasks such as Video Question Answering (VQA), Video Captioning (VC), and Relation Reasoning (RR).

In this paper, we propose the Multimodal LLMs on a Scene HyperGraph (HyperGLM) approach to promote *reasoning about multi-way interactions and higher-order relationships* through a unified HyperGraph and LLMs, as illustrated in Fig. 1. To achieve this goal, we uniquely incorporate *entity scene graphs*, which capture spatial relationships between objects, with a *procedural graph* that models their causal transitions across video frames, forming a *unified HyperGraph*, as shown in Fig. 2. Significantly, our HyperGLM approach allows reasoning by injecting this unified HyperGraph into LLMs. In addition, we introduce a novel Video Scene Graph Reasoning (VSGR) dataset, comprising 1.9 million video frames surpassing existing benchmark datasets [18, 34, 35, 47, 52] in scale and annotation depth. Specifically, our VSGR dataset includes videos from third-person, egocentric, and drone perspectives. It supports five tasks: Scene Graph Generation, Scene Graph Anticipation, Video Question Answering, Video Captioning, and Relation Reasoning. Notably, our VSGR dataset introduces a new *Relation Reasoning* task, setting it apart from existing video scene graph datasets, as shown in the comparison in Table 1.

Contributions of this Work. This work presents three contributions to advance Video Scene Graph Generation. First, we introduce Multimodal LLMs on a Scene HyperGraph, leveraging hyperedges and LLMs for *reasoning about multi-way interactions and higher-order relationships*. Second, we develop a new Video Scene Graph Reasoning dataset, surpassing existing scale and annotation depth benchmarks. Our VSGR dataset primarily supports five tasks within diverse video scenes. Finally, the proposed HyperGLM consistently outperforms state-of-the-art methods across all five tasks.

2. Related Work

In this section, we review advances in scene graph generation and hypergraph applications in computer vision, then discuss existing limitations and the advantages of our approach.

2.1. Scene Graph Generation

Scene Graph Generation has significantly advanced with transformer-based models [6, 13, 17, 25, 26, 51] that have become benchmarks due to their efficiency and state-of-the-art performance. Recent work [3, 21, 33] focuses on reducing bias and enhancing mean recall for rare predicates by integrating external knowledge and applying unbiased contextual augmentation, particularly in dynamic video contexts. Open-vocabulary methods [15, 27] supported by vision-language models handle unseen object and relationship classes, improving generalization. Additionally, generative models (e.g., diffusion-based methods [9, 53]) leverage scene graphs for efficient image and scene synthesis. More-

over, spatial-temporal methods [4, 34–36, 42] effectively capture dynamic object relationships in videos. Recently, Large Language Models [23] have been utilized to enhance triplet extraction and alignment in weakly supervised SGG.

2.2. HyperGraphs

HyperGraphs have been adopted in computer vision to model complex multimodal data and capture higher-order relationships. Unlike traditional graph-based approaches, HyperGraphs connect multiple nodes through hyperedges, enabling multi-way relationships. They enhance Graph Neural Networks (GNNs) [12, 54] by allowing the modeling of more sophisticated interactions. Recent advancements, such as HyperGraph Convolution [1] and HyperGraph Attention [22], have further improved GNNs by capturing relationships beyond simple pairwise connections. Therefore, HyperGraph-based models effectively handle temporal dependencies and complex interactions, significantly boosting performance in tasks like accident anticipation [43], group activity recognition [28, 55], and video question answering [44, 46, 50].

2.3. Discussion

Limitations in Prior Methods. The methods introduced in Section 2.1, based on *Progressive Feature Fusion* [39, 51], *Batch-Progressive Transformer Encoding* [6, 13, 17, 25, 26], *Spatial-Temporal Context Integration* [4, 34, 42], and *Memory-Guided Temporal Consistency* [7, 33, 35], have advanced VidSGG. However, these methods struggle to model *higher-order relationships* and complex temporal dynamics. Specifically, *Progressive Feature Fusion* and *Batch-Progressive Transformer Encoding* are limited in capturing long-term temporal dependencies, with the former lacking long-term context due to frame-by-frame processing and the latter only addressing short-term dependencies. Similarly, *Spatial-Temporal Context Integration* and *Memory-Guided Temporal Consistency* inadequately represent multi-object interactions across video frames and insufficiently capture the temporal evolution required for higher-order relationships.

Advantages of Our Approach. Our HyperGLM approach, Multimodal LLMs on a Scene HyperGraph, promotes *reasoning about multi-way interactions and high-order relationships*. As illustrated in Fig. 2, HyperGLM enhances the model’s ability to interpret complex relationships and anticipate intricate video dynamics. Towards this goal, we uniquely integrate *entity scene graphs*, which is introduced in Sec. 3 to capture spatial interactions between objects in each frame and a *procedural graph*, which is presented in Sec. 4.1 to model their causal evolution. In our unified approach, hyperedges connect multiple nodes to capture higher-order relationships distinguished from traditional pairwise methods [4, 34, 35, 42]. In addition, the procedural graph enables *multi-step transitions* for anticipating future interactions or relationships, and *reduces bias* by generalizing

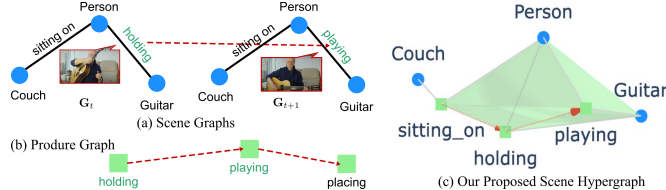


Figure 2. (a) To model the temporal transition, a simple approach can be using two scene graphs G_t and G_{t+1} . (b) Another procedure graph can present this temporal modeling. (c) Our unified HyperGraph in Fig. 2c integrates both *entity scene graph* to capture spatial relationships and the *procedural graph* to model the temporal evolution. *HyperEdge* represents *person holding*, *holding playing*, whereas *holding* → *playing* describes a chain of interactions. HyperGraph is presented in 3D.

infrequent relationship categories. Furthermore, our HyperGLM approach leverages fundamental mathematical properties: *permutation equivariance* ensures that the HyperGraph structure remains consistent under any permutation of node labels, and *invariance to hyperedge order* preserves semantic meanings regardless of the node visit order during random walks which is defined in Alg. 1. The theoretical foundations and mathematical properties are detailed in the **Appendices**.

3. Problem Formulation

In this section, we define two tasks, including Scene Graph Generation (SGG) and Scene Graph Anticipation (SGA). Graph vertex sequence is represented as $\{V_G \mid 1 \leq t \leq T\}$, where each set of vertex V_G contains object features, bounding boxes, and categories. The scene graph for each frame t , denoted by $G_t = (V_G, E_G = \{r^{ij} \mid 1 \leq i < j \leq |V_G|\})$, consists of all pairwise relationships between objects, with r^{ij} representing the relationship category between v_i and v_j .

We aim to develop a process $p_\theta : (V_G \times V_G) \rightarrow r^{ij}$ to predict the relationship r^{ij} between each object pair (v_t^i, v_t^j) in V_G . We define task-specific queries Q_{SGG} , and Q_{SGA} to direct our unified model to perform on each specific task. The objective for each task is to minimize the negative likelihood of the predicted scene graph G_t to the truth predicate set $Y_t = \{y_k^{ij} \mid 1 \leq i < j \leq |V_G|\}$ on categories indexed by k . **Scene Graph Generation (SGG)** generates the scene graph for each frame t from $t = 1$ to $t = T$, which is defined as:

$$\min_{\theta} \mathbb{E}_{G_t, Y_t} \left[- \sum_{(v_t^i, v_t^j)} \sum_k (y_k^{ij} \log p_\theta(r^{ij} \mid Q_{SGG})_k) \right] \quad (1)$$

Scene Graph Anticipation (SGA) anticipates the scene graphs for future frames, generating predictions G_{t+n} , where n denotes the anticipation horizon, formulated as:

$$\min_{\theta} \mathbb{E}_{G_{\leq t}, Y_t} \left[- \sum_{(v_{t+n}^i, v_t^j)} \sum_k (y_k^{ij} \log p_\theta(r^{ij} \mid Q_{SGA})_k) \right] \quad (2)$$

In Eqns. (1) and (2), t indexes the current frame. While SGG predicts the scene graph at frame t , SGA reads scene graphs up to frame t to forecast the graph in future frame $t + n$.

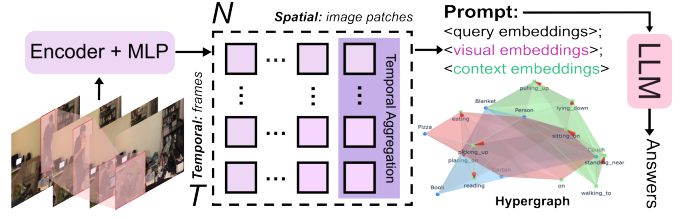


Figure 3. Our HyperGLM framework comprises an image encoder, MLP projector, temporal aggregator, unified HyperGraph, and language model. It processes video frames by encoding each frame with the image encoder and MLP, extracting spatio-temporal features through image patch grids to generate N spatial tokens per frame. The temporal aggregator compresses the $T \times N$ embeddings over time. The MLP projector then transforms these visual embeddings into the language feature space as frame tokens, interleaved with language tokens, and fed into the Large Language Models.

4. Our Proposed HyperGLM Approach

In this section, we present our approach, which incorporates a unified HyperGraph into the LLMs, as illustrated in Fig. 3.

4.1. Video Scene (Hyper)Graphs

Traditional VidSGG methods [4, 34, 42] construct scene graphs G_t to represent *scene entities* and *their relationships* as in Fig. 2a. However, these graph-based approaches do not capture *higher-order relationships with temporal dependencies* for video understanding [36]. To model this property, we propose a novel HyperGraph-based framework that constructs a unified HyperGraph $\mathcal{H} = (V_H, E_H)$, representing spatial relationships within individual frames and temporal transitions across frames, illustrated in Fig. 4. HyperGraph extends traditional graph structures by allowing hyperedges to connect more than two nodes, making them particularly effective for modeling these higher-order relationships. To leverage this property, our unified HyperGraph (see Fig. 2c) integrates *entity scene graphs* G_t for each frame, capturing spatial interactions as introduced in Sec. 3, along with a *procedural graph* P that models their causal transitions, as detailed in Sec. 4.1. We unify these components using a *random-walk HyperGraph construction*, which is defined in Alg. 1 to capture higher-order connectivity patterns and structural semantics, thereby approximating subgraph matching between the entity scene graphs and the procedural graph. This integration allows our approach to model current subjects' interactions and anticipate their future relationships.

Procedural Graph Construction. SGA objective is to predict the set of relationships E_G in the next frame based on the current set of relationships. To model the temporal evolution of causal relationships between objects across video frames, we introduce a *procedural graph* $P = (V_P, E_P)$, serving as the temporal counterpart to the entity scene graphs G_t as shown in Fig. 2b. In particular, the procedural graph P can vary across datasets, modeling relationship transitions.

Toward this goal, we model and denote the set of vertices in P as $V_P = \{r_t^{ij} \in V_G \mid 1 \leq t \leq T\}_\neq$, representing *distinct relationship categories*. The set of edges in P , i.e.,

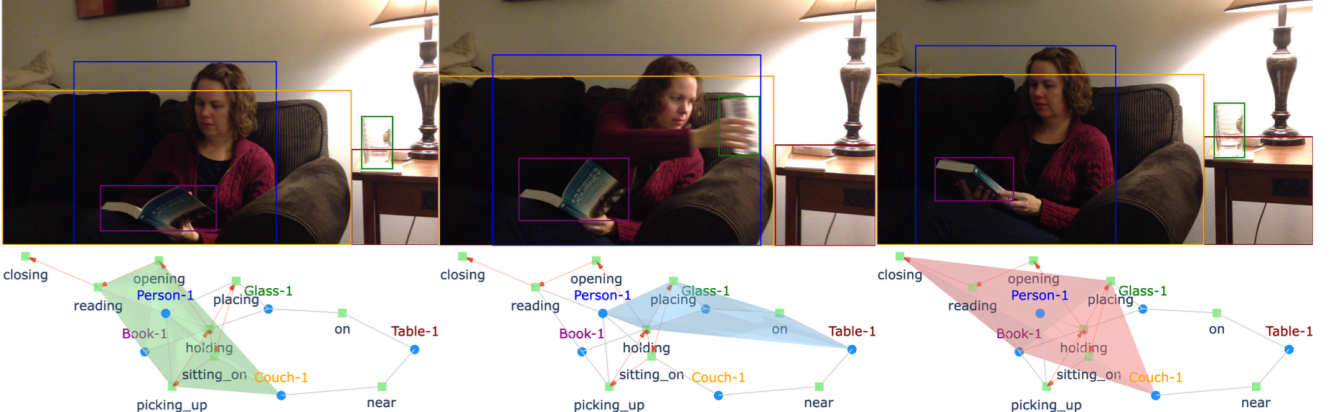


Figure 4. Our Video Scene HyperGraph, including *entity graphs* and a *procedural graph*, as defined in Sec. 4.1. Blue nodes represent **entities**, while green nodes denote **relationships**. The entity graph captures spatial relationships ($\text{subject} \multimap \text{relationship} \multimap \text{object}$), whereas the procedural graph models relationship transitions (\rightarrow). *Hyperedges* are visualized as polygons, encapsulating interactions through chains of relationships. For instance, a hyperedge illustrates a person picking up, holding, opening, and reading a book while sitting on a couch. HyperGraph is presented in 3D, see *Supplementary video*.

$E_{\mathbf{P}} = \{(r_m, r_n)\}$ represent possible *causal transitions between these relationships*, where an edge (r_m, r_n) indicates that relationship r_m causally lead to relationship r_n . We quantify causal transitions by calculating transition probabilities $w(r_m, r_n)$ via their observed frequencies as in Eqn. (3).

$$w(r_m, r_n) = \frac{\sum_{t=1}^{T-1} \sum_{r_{t,t+1}^{ij}} \mathbb{1}(r_t^{ij} = r_m \wedge r_{t+1}^{ij} = r_n)}{\sum_{t=1}^{T-1} \sum_{r_{t,t+1}^{ij}} \mathbb{1}(r_t^{ij} = r_m)} \quad (3)$$

where $\mathbb{1}(\cdot)$ is the indicator function that counts transitions from relationship r_m at current frame t to r_n at next frame $t + 1$. Next, self-loops $w(r_m, r_m)$ are removed from the graph, and these probabilities are normalized as in Eqn. (4).

$$\sum_{r_n \in E_{\mathbf{P}}} w(r_m, r_n) = 1 \quad \text{for all } r_m \in E_{\mathbf{P}} \quad (4)$$

By leveraging these probabilities, the procedural graph \mathbf{P} enhances the prediction of future relationships. For each relationship r_t^{ij} in frame t , the most probable relationship r_{t+1}^{ij} in the next frame $t + 1$ is determined as in Eqn. (5).

$$r_{t+1}^{ij} = \arg \max_{r_n} P(r_n | r_t^{ij}, v^{i,j}) \quad (5)$$

where $P(r_n | r_t^{ij}, v^{i,j}) = w(r_t^{ij}, r_n) \times v^{i,j}$ is the probability of transitioning from relationship r_t^{ij} to r_n , looking at object features. This allows the model to anticipate future interactions based on established temporal patterns.

HyperGraph Construction. To incorporate spatial relationships between objects in each frame and their causal temporal transitions, we construct a unified HyperGraph \mathcal{H} that integrates the *entity scene graphs* \mathbf{G}_t and the *procedural graph* \mathbf{P} . Specifically, a HyperGraph is an augmented

representation combining the entity scene graphs with the procedural graph. This unified structure merges spatial and temporal relationships into a single graph, enabling the use of conventional graph algorithms while preserving the complex interactions captured by the HyperGraph. Mathematically, a unified HyperGraph $\mathcal{H} = (V_{\mathcal{H}}, E_{\mathcal{H}})$ is defined as in Eqn. (6).

$$\mathcal{H} = \left(\bigcup_{t=1}^T V_{\mathbf{G}_t} \cup V_{\mathbf{P}}, \quad \bigcup_{t=1}^T E_{\mathbf{G}_t} \cup E_{\mathbf{P}} \right) \quad (6)$$

where $V_{\mathcal{H}}$ includes all entity nodes v_t^i from each \mathbf{G}_t and the relationship type nodes $V_{\mathbf{P}}$. The hyperedge set $E_{\mathcal{H}}$ includes pairwise relationships $E_{\mathbf{G}_t}$ within each \mathbf{G}_t , capturing spatial relationships and temporal transition edges $E_{\mathbf{P}}$ from \mathbf{P} , modeling the evolution of causal relationships across frames.

Random-walk Algorithm. We employ the random walks algorithm outlined in Alg. 1 to sample representative substructures from the unified HyperGraph \mathcal{H} , which captures connectivity patterns and mitigates the NP-hardness of exact subgraph matching. Specifically, these walks alternate between nodes and hyperedges, preserving the multi-node connections intrinsic to hyperedges and capturing the complexity of multi-object relationships and their transition across video frames. In each walk, a hyperedge h_i aggregates the visited nodes, thereby encapsulating higher-order relationships. For example, in the entity scene graph \mathbf{G}_t , a walk might traverse from a ‘‘person’’ to a ‘‘cup’’ via the ‘‘holding’’, resulting in the hyperedge $h_i = \{\text{person}, \text{cup}\}$. Similarly, within the procedural graph \mathbf{P} , a walk might transition through a sequence of interactions such as ‘‘holding’’, ‘‘placing’’, and ‘‘releasing’’, forming the hyperedge $h_i = \{\text{holding}, \text{placing}, \text{releasing}\}$. Therefore, we generate sampled hyperedges $E_{\text{sampled}} = \{h_i | i = 1, \dots, N_w\}$ as in L25 of Alg. 1 by conducting multiple random walks.

Algorithm 1 Random-walk for HyperGraph Construction.

Require: $\mathcal{H} = (V_{\mathcal{H}}, E_{\mathcal{H}})$, Number of Walks N_w , Walk Length N_l

Ensure: $\mathcal{H}' = (V_{\mathcal{H}}, E'_{\mathcal{H}})$

- 1: Initialize $E_{\text{sampled}} \leftarrow \emptyset$
- 2: **for** $i = 1$ to N_w **do**
- 3: Select $v_{\text{start}} \in V_{\mathcal{H}}$ uniformly at random
- 4: Initialize walk sequence $S \leftarrow [v_{\text{start}}]$
- 5: **for** $j = 1$ to N_l **do**
- 6: **if** j is odd **then** \triangleright Node to HyperEdge
- 7: $v_{\text{current}} \leftarrow S[j]$
- 8: $\mathcal{E}_{v_{\text{current}}} \leftarrow \{h \in E_{\mathcal{H}} \mid v_{\text{current}} \in h\}$
- 9: **if** $\mathcal{E}_{v_{\text{current}}} \neq \emptyset$ **then**
- 10: Select $h_j \in \mathcal{E}_{v_{\text{current}}}$
- 11: Append h_j to S
- 12: **end if**
- 13: **else** \triangleright HyperEdge to Node
- 14: $h_{\text{current}} \leftarrow S[j]$
- 15: $V_{h_{\text{current}}} \leftarrow h_{\text{current}}$
- 16: Select $v_j \in V_{h_{\text{current}}}$
- 17: Append v_j to S
- 18: **end if**
- 19: **end for**
- 20: $h_i \leftarrow \{v \in S \mid v \in V_{\mathcal{H}}\}$ \triangleright Form new HyperEdge
- 21: **if** $h_i \notin E_{\mathcal{H}} \cup E_{\text{sampled}}$ **then**
- 22: $E_{\text{sampled}} \leftarrow E_{\text{sampled}} \cup \{h_i\}$
- 23: **end if**
- 24: **end for**
- 25: $E'_{\mathcal{H}} \leftarrow E_{\mathcal{H}} \cup E_{\text{sampled}}$
- 26: **return** $\mathcal{H}' = (V_{\mathcal{H}}, E'_{\mathcal{H}})$

4.2. Multimodal LLMs on HyperGraphs

Formulation. Given an input video \mathbf{V} and a task query \mathbf{Q} , we aim to generate a target answer sequence \mathbf{A} of length L . Especially, by modeling a HyperGraph \mathcal{H} , the target answer \mathbf{A} is generated via a process illustrated in Fig. 3, defined as:

$$p(\mathbf{A}|\mathbf{V}, \mathbf{Q}, \mathcal{H}) = \prod_{i=0}^{L-1} p(x_i|\mathbf{V}, \mathbf{Q}, \mathcal{H}, x_{<i}) \quad (7)$$

where $x_{<i}$ denotes the preceding token sequence, and $\mathbf{A} = [x_0, \dots, x_i, \dots, x_{L-1}]$ is the sequence of answer tokens reasoning video \mathbf{V} by question \mathbf{Q} and HyperGraph \mathcal{H} in Fig. 4.

As illustrated in Fig. 5, our process begins with the *generation*, constructing an entity scene graph $\mathbf{G}_t = (V_t^e, E_{\mathbf{G}})$ for each frame t to capture detected objects and their relationships. *Relationship anticipation* employs the procedural graph \mathbf{P} to model temporal evolution and predict future interactions. The model then engages in *reasoning* using the HyperGraph \mathcal{H} and *verification* through video captioning to ensure contextual relevance and accuracy. It refines understanding through *clarification*, generating answers by reasoning over the video and \mathcal{H} . In *scene forecasting*, it predicts

Table 1. Comparisons of video scene graph datasets. SGG, SGA, VQA, VC, and RR represent Scene Graph Generation, Scene Graph Anticipation, Video Question Answering, Video Captioning, and Relation Reasoning.

Dataset	#Frames	Tasks					Annotations		
		SGG	SGA	VQA	VC	RR	Bbox	Relation	Text
SportsHHI [47]	11.4K	✓	✗	✗	✗	✗	✓	✓	✗
Action Genome [18]	234.3K	✓	✓	✗	✗	✗	✓	✓	✗
AeroEye [35]	261.5K	✓	✗	✗	✗	✗	✓	✓	✗
ASPIRe [34]	1.6M	✓	✗	✗	✗	✗	✓	✓	✗
PVSG [52]	153K	✓	✗	✓	✓	✗	✓	✓	✓
VSGR (Ours)	1.9M	✓	✓	✓	✓	✓	✓	✓	✓

subsequent interactions by identifying new relationships and adapting to evolving contexts using transition probabilities in \mathbf{P} , anticipating future relationships r_{t+n}^{ij} and improving conversational flow. Finally, the *hypothesis* allows the model to propose and test conjectures about the underlying themes or intentions, synthesizing information from previous steps and leveraging \mathcal{H} to explain patterns and forecast results.

5. Video Scene Graph Reasoning Dataset

Limitations of Current Datasets. Existing benchmarks (see Table 1) primarily support SGG and SGA, limiting their applicability to reasoning tasks. They suffer from inadequate support for VQA, VC, and RR, shallow annotations that fail to capture intricate object interactions, insufficient modeling of temporal dynamics, and poor multimodal integration. Thus, our VSGR dataset supports SGG, SGA, VQA, VC, and RR, enabling the reasoning capabilities of LLMs.

5.1. Dataset Construction

Data Acquisition Stage. We source videos from the ASPIRe [34] and AeroEye [35] datasets. While the ASPIRe dataset offers diverse, richly annotated videos emphasizing dynamic interactions and temporal changes, the AeroEye dataset offers drone-captured footage across various scenes. **Comprehension Tasks via Question-Answering.** We introduce tasks that leverage fine-grained relationships from scene graphs, extending Scene Graph Generation to focus on relation understanding and subject/object interpretation using $\langle \text{subject}, \text{relation}, \text{object} \rangle$ triplets and leverage GPT-4/GPT-3.5 model for language generation.

Video Captioning (VC). We generate 82,532 video-caption pairs, resulting in about 22 captions per video. Our process involves (1) extracting triplets from cropped video frames focusing on foreground objects, (2) generating background descriptions based on these triplets, and (3) combining the foreground triplets and background descriptions to produce captions. The average length is 893 characters, surpassing the PVSG [52] dataset in quantity and detail.

Video Question Answering (VQA). We develop 74,856 question-answer pairs by designing questions that explore diverse relationships, selecting subject and object categories to verify specific relationships, or choosing triplets to assess their uniqueness. This results in an average of approximately 20 questions per video, which exceeds existing benchmarks



Figure 5. An example of the diversified context within the streaming dialog in our VSGR dataset. **Best viewed in color and zooming in.**

such as the MSRVTT-QA [49] and MSVD-QA [48] datasets.

Relation Reasoning (RR). Using the annotated scene graphs, we produce 61,120 relation reasoning tasks by selecting partial information as an incomplete input. Each task requires the model to deduce relationships among entities and identify the categories of the subject and object. With an average of approximately 16 tasks per video, our VSGR dataset provides a substantial collection for evaluating models’ abilities in relational reasoning and scene understanding.

Question and Answer Validation. To ensure the quality and complexity of questions, we implement a rigorous validation process that combines generation by LLMs with human refinement. Initially, GPT-4/GPT-3.5 generates queries based on the $\langle \text{subject}, \text{relation}, \text{object} \rangle$ triplets extracted from the videos. Human annotators are trained with specific guidelines that emphasize clarity, relevance, and appropriate challenge levels, then review and refine questions. They enhance the questions by ensuring they are directly answerable from the video content and require careful reasoning about the depicted interactions and relationships.

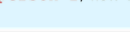
We apply strict filtering criteria to improve the quality of the dataset. First, we eliminate questions that do not require video context and can be answered using general world knowledge, ensuring that models must rely on visual information from the videos. Second, we exclude questions that LLMs can answer correctly, increasing the challenge and utility of the dataset in evaluating advanced reasoning abilities. Finally, independent annotators perform a second round to review and evaluate the quality of the refined questions.

Step-4: Verification

Does **person-1** move towards **ball-2** and begin dribbling, and does **person-2** start practicing shots with **ball-1** through ?

Yes, both individuals are focused on separate balls. **person-1** continues with **ball-1**, and **person-2** remains with **ball-2**, indicating individual practice rather than switching activities or interacting with each other.

Step-5: Clarification

If instead, **person-1** picks up **ball-2** and passes it to **person-2**, how would that change the dynamics of ?

This would shift the dynamics from individual practice to a collaborative activity, with **person-1** passing **ball-2** to **person-2**. The interaction would signal the start of coordinated play, possibly initiating a game involving both **ball-1** and **ball-2** and highlighting teamwork between **person-1** and **person-2**.

Step-6: Scene Forecasting

Given , what are the likely relationship changes between objects in the upcoming phase?

The next action could involve **person-1** passing **ball-2** to **person-2** while **person-2** passes **ball-1** to **person-1**. Alternatively, **person-1** might dribble **ball-2** toward **person-2**, initiating a one-on-one game.

Step-7: Hypothesis

What if **person-3** [600, 200, 160, 500] enters  and approaches the others? How might that affect the interactions?

person-1, **person-2**, and **person-3** could engage in coordinated actions, such as three-person passing drills using **ball-1** and **ball-2**. The interaction would evolve from individual practice to collaborative teamwork.

5.2. Dataset Comparison

As reported in Table 1, our VSGR dataset represents a substantial advancement in video scene graph benchmarks. Our dataset comprises 3,748 videos and 1,841,243 frames, surpassing existing datasets in scale. Unlike other datasets that address only a limited subset of tasks, our dataset offers comprehensive task coverage, facilitating multifaceted evaluations of LLMs. In addition, our ground truth enriches relation annotations with comprehensive textual descriptions, enabling sophisticated reasoning and relationship predictions, as illustrated in Fig. 5. Additionally, our VSGR dataset incorporates diverse viewpoints, including third-person, ego-centric, and drone perspectives, enhancing its generalization.

6. Experiment Results

6.1. Implementation Details

Datasets. We leverage our VSGR dataset across five tasks. In addition, we utilize the PVSG [52] dataset for the SGG task and the Action Genome [18] dataset for the SGA task.

Model Configuration. We operate the CLIP-ViT-L-336 [8, 37] to encode each video frame into ten tokens (one CLS token and nine from 3×3 average pooling). These tokens are fed into a two-layer MLP connector to the Mistral-7B-Instruct [19] language model. For training, we apply LoRA [16] to all linear layers with a rank of 128 and a scaling factor of 256, omitting vision-language alignment [31]. We train for two epochs with a batch size of 128 over 16

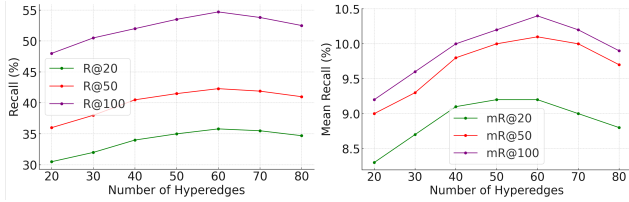


Figure 6. Comparison of Recall (R) and mean Recall (mR) at different numbers of hyperedges for the SGG task on the VSGR dataset.

Table 2. Comparison (%) on the VSGR and Action Genome datasets for the Scene Graph Anticipation (SGA) task at varying video input fractions \mathcal{F} .

\mathcal{F}	Method	Action Genome			VSGR		
		R/mR@10	R/mR@20	R/mR@50	R/mR@10	R/mR@20	R/mR@50
0.3	STTran+ [5]	13.9 / 3.5	21.6 / 7.3	40.8 / 20.3	12.0 / 4.0	19.0 / 8.0	35.7 / 18.0
	DSGDetr+ [11]	14.3 / 3.6	21.8 / 7.6	41.3 / 21.2	12.5 / 4.2	19.5 / 8.3	36.0 / 19.0
	STTran++ [5]	15.4 / 6.2	27.2 / 14.1	48.6 / 32.2	14.0 / 6.5	22.0 / 11.0	39.0 / 25.1
	DSGDetr++ [11]	16.8 / 8.4	29.0 / 16.7	48.9 / 32.3	14.5 / 7.0	22.5 / 12.0	40.0 / 26.0
	SceneSayerODE [36]	23.3 / 13.3	32.5 / 20.1	45.1 / 33.0	18.0 / 9.5	26.0 / 15.0	42.0 / 30.0
	SceneSayerSDE [36]	25.9 / 15.6	35.7 / 23.1	47.4 / 37.1	19.5 / 11.0	27.5 / 17.0	44.0 / 33.5
	HyperGraph (Ours)	26.5 / 14.8	36.2 / 22.1	49.3 / 37.2	18.8 / 9.3	27.2 / 16.3	42.5 / 27.4
	HyperGLM (Ours)	27.5 / 15.8	37.0 / 24.5	50.0 / 38.0	19.0 / 10.0	28.0 / 16.5	43.0 / 37.5
0.5	STTran+ [5]	14.9 / 3.7	22.6 / 7.6	42.9 / 21.4	13.5 / 4.2	21.0 / 8.5	37.0 / 19.0
	DSGDetr+ [11]	15.2 / 3.9	23.1 / 8.0	43.3 / 22.2	13.8 / 4.5	21.5 / 9.0	38.0 / 20.0
	STTran++ [5]	16.6 / 6.6	29.1 / 14.7	51.5 / 33.4	15.5 / 7.0	23.5 / 12.5	41.0 / 26.5
	DSGDetr++ [11]	17.4 / 8.4	30.5 / 17.0	51.9 / 33.9	16.0 / 7.5	24.0 / 13.0	42.0 / 28.0
	SceneSayerODE [36]	26.4 / 14.3	36.6 / 21.4	49.8 / 36.0	20.5 / 11.0	29.5 / 16.5	46.1 / 32.5
	SceneSayerSDE [36]	28.4 / 16.3	38.6 / 25.1	51.4 / 39.9	21.5 / 12.5	31.0 / 18.5	48.0 / 35.7
	HyperGraph (Ours)	29.2 / 16.4	39.3 / 23.2	52.1 / 38.7	20.3 / 12.2	29.8 / 17.1	46.2 / 33.1
	HyperGLM (Ours)	30.0 / 17.0	40.5 / 27.5	53.5 / 40.5	21.5 / 11.5	31.5 / 18.5	46.5 / 36.0
0.7	STTran+ [5]	16.6 / 4.2	25.1 / 8.5	47.2 / 24.0	15.0 / 5.0	24.0 / 10.5	41.0 / 21.5
	DSGDetr+ [11]	16.8 / 4.3	25.3 / 8.8	47.4 / 24.7	15.5 / 5.2	24.5 / 11.0	42.0 / 22.0
	STTran++ [5]	19.0 / 7.7	32.8 / 17.1	56.8 / 36.8	17.0 / 8.0	27.0 / 14.0	45.0 / 29.0
	DSGDetr++ [11]	19.8 / 9.5	34.1 / 19.2	56.7 / 37.2	17.5 / 8.5	28.0 / 15.0	46.1 / 30.0
	SceneSayerODE [36]	32.1 / 16.5	42.8 / 24.4	55.6 / 39.6	23.5 / 13.0	33.5 / 19.0	51.0 / 36.0
	SceneSayerSDE [36]	33.3 / 18.1	44.0 / 27.3	56.4 / 44.4	24.5 / 14.5	35.7 / 21.0	53.0 / 38.0
	HyperGraph (Ours)	34.3 / 19.2	45.2 / 25.3	57.2 / 42.1	22.3 / 13.2	34.2 / 19.3	50.4 / 38.3
	HyperGLM (Ours)	35.7 / 19.5	46.1 / 30.0	58.2 / 44.0	25.1 / 13.5	35.5 / 21.5	51.0 / 33.5

iterations on $4 \times$ GPUs, taking approximately six hours.

Metrics. We evaluate the SGG and SGA tasks using the Recall and mean Recall scores. In addition, we evaluate the VQA and RR tasks by Accuracy, Precision, Recall, and F1 scores. For the VC task, we utilize CIDEr, MENTOR, ROUGE-L, and BLEU-4 scores to validate our performance.

Settings. For the SGG and SGA tasks, we adopt the evaluation settings based on [18, 36]. In particular, the model is provided with raw video frames and must detect objects using a pre-trained detector (*i.e.* Faster R-CNN) and predict or anticipate their relationships. Especially for the SGA, we set the initial video input fraction (\mathcal{F}) to 0.9, following [36].

6.2. Ablation Study

Hypergraph Parameters. The number of walks (N_w) and walk length (N_l) are introduced in Alg. 1, directly impacting the capacity to capture high-order relationships by determining the number of hyperedges. Although more hyperedges increase relational diversity, they can also introduce redundancy beyond an optimal point. Specifically, a higher N_w broadens the range of sampled relationships, while a moderate N_l balances depth. Our experiments demonstrate that optimal performances are achieved with 60 hyperedges ($N_w = 60$ and $N_l = 7$), shown in Fig. 6. Further experiments on the SGG task are provided in Table 3, and experiments on these parameters are included in the Appendices.

Video Input Fraction. We adjust the initial video input

Table 3. Comparison (%) on the VSGR and PVSG datasets for the Scene Graph Generation (SGG) task at Recall (R) and mean Recall (mR).

Method	PVSG			VSGR		
	R/mR@20	R/mR@50	R/mR@100	R/mR@20	R/mR@50	R/mR@100
Transformer [52]	4.0 / 1.8	4.4 / 1.9	4.9 / 2.0	25.7 / 6.3	34.5 / 6.5	43.5 / 7.0
HIG [34]	4.6 / 1.9	4.9 / 2.1	5.4 / 2.2	23.8 / 5.7	31.1 / 5.9	40.4 / 6.9
CYCLO [35]	5.8 / 2.0	6.1 / 2.2	6.7 / 2.3	29.4 / 7.1	36.4 / 7.7	47.7 / 7.7
HyperGraph (Ours)	6.5 / 2.2	7.0 / 2.4	7.5 / 2.6	31.6 / 7.8	38.8 / 8.3	50.3 / 8.5
HyperGLM (Ours)	7.5 / 2.8	8.1 / 3.7	8.5 / 3.9	35.8 / 9.2	42.3 / 10.1	54.7 / 10.4

Table 4. Comparison (%) on the VSGR and Action Genome datasets for the Scene Graph Anticipation (SGA) task at Recall (R) and mean Recall (mR).

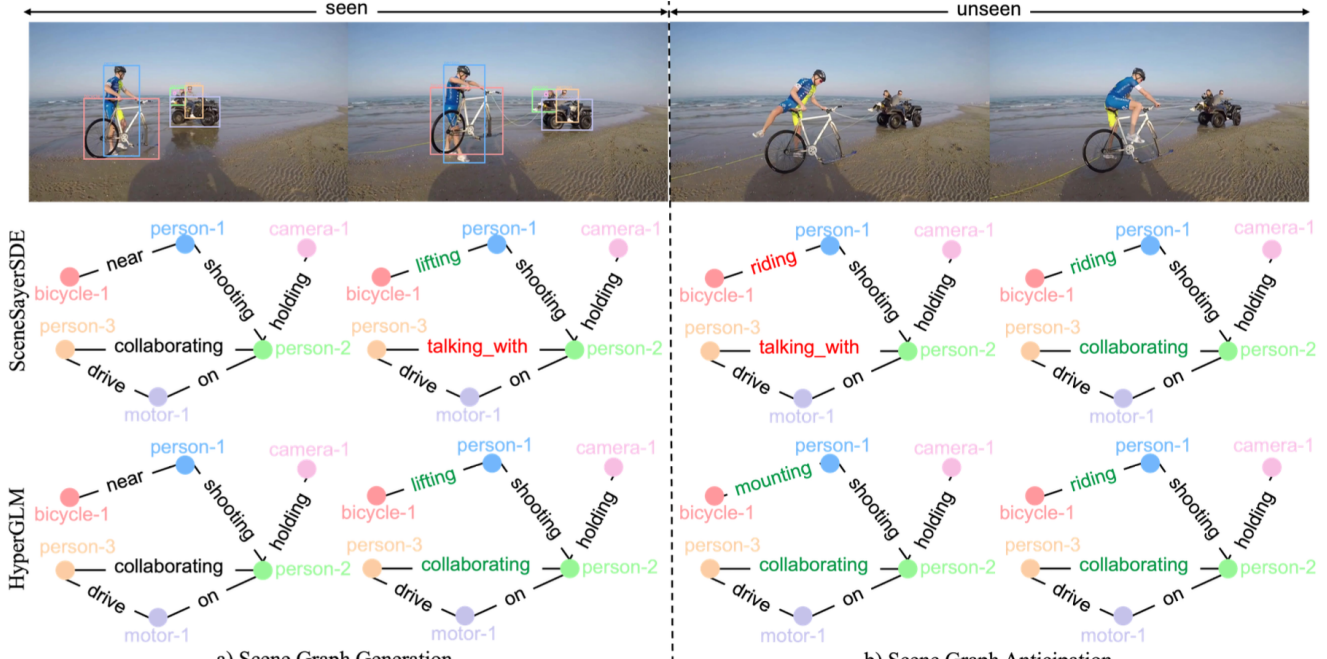
Method	Action Genome			VSGR		
	R/mR@10	R/mR@20	R/mR@50	R/mR@10	R/mR@20	R/mR@50
STTran+ [5]	17.5 / 4.6	26.8 / 9.2	49.6 / 24.3	16.5 / 5.5	26.0 / 11.0	43.0 / 23.0
DSGDetr+ [11]	17.9 / 4.7	27.7 / 9.7	51.4 / 25.9	17.0 / 6.0	27.0 / 11.5	44.5 / 24.5
STTran++ [5]	20.2 / 8.9	35.7 / 18.4	60.2 / 38.8	19.0 / 9.5	30.0 / 15.5	49.0 / 31.0
DSGDetr++ [11]	22.2 / 11.4	37.1 / 21.0	61.0 / 39.5	19.5 / 10.0	31.0 / 16.0	50.0 / 32.5
SceneSayerODE [36]	36.6 / 17.8	48.3 / 27.4	61.3 / 43.4	26.5 / 14.0	37.5 / 20.0	55.5 / 38.0
SceneSayerSDE [36]	37.3 / 20.8	48.6 / 30.9	61.6 / 46.8	27.5 / 16.0	38.5 / 22.0	58.2 / 40.0
HyperGraph (Ours)	37.5 / 19.1	49.3 / 31.4	62.3 / 47.4	28.4 / 17.5	39.3 / 22.4	57.6 / 41.5
HyperGLM (Ours)	38.8 / 22.3	51.5 / 33.0	65.2 / 48.6	30.2 / 18.1	41.1 / 23.5	59.3 / 43.4

fraction, \mathcal{F} , to 0.3, 0.5, and 0.7 for the SGA task. This adjustment allows the model to learn from varying observed portions and predict the unseen segment. Table 2 indicates that increasing the portion of the seen video improves performance, suggesting that additional visual context is beneficial. In addition, Table 4 further confirms that the default setting at a higher input fraction ($\mathcal{F} = 0.9$) leads to optimal performance. We also present additional settings with varying video input fractions for the SGA task in the Appendices.

6.3. Comparison with State-of-the-Arts

Table 3 demonstrates that HyperGLM significantly outperforms existing methods on the PVSG and VSGR datasets, achieving the highest R@20 scores of 7.5% and 35.8%, respectively. By leveraging hyperedges connecting multiple nodes within the HyperGraph, HyperGLM effectively captures complex object interactions and spatial dependencies, transcending traditional pairwise methods to generate more accurate and detailed scene graph representations. Notably, integrating a procedural graph within the HyperGraph *reduces bias*. Our approach enhances mean Recall, reaching improvements of 2.8% on the PVSG dataset and 9.2% on the VSGR dataset, thereby addressing the long-tail distribution challenges that have struggled in previous methods [34, 35, 52]. Furthermore, the LLM enhances the capacity of HyperGLM to infer and predict intricate relationships embedded within the unified HyperGraph, resulting in improved performance compared to HyperGraph, which shows a decrease of 4.2% at R@20 on the VSGR dataset.

As shown in Table 4, our HyperGLM approach outperforms existing SGA methods on the Action Genome and VSGR datasets, achieving R@10 scores of 35.7% and 25.1%, respectively. This improvement stems from integrating procedural graphs that model *causal relationships* within the HyperGraph structure. In contrast, the SceneSayer [36] method relies on NeuralODE and NeuralSDE to capture the latent dynamics of object interaction evolution. Our procedural graphs enable *multi-step transitions* that explicitly



a) Scene Graph Generation

Figure 7. Qualitative comparison of our HyperGLM approach versus SceneSayerSDE [36] for SGG and SGA. Red and green edge labels denote incorrect and correct predictions, respectively. Our HyperGLM approach effectively captures the evolving interactions between **person-1** and **bicycle-1** or **person-2** and **person-3** over time and anticipates interactions in unseen video frames, while SceneSayerSDE confuses to similar predicates. **Best viewed in color.**

Table 5. Comparison (%) on VSGR for the Video Question Answering.

Method	Accuracy	Precision	Recall	F1 Score
Video-ChatGPT [32]	33.2	35.1	32.3	33.6
Video-LLaVA-7B [30]	43.1	43.8	41.7	42.7
MovieChat [41]	43.5	44.2	42.6	43.4
Chat-UniVi-7B [20]	44.3	45.6	43.2	44.4
HyperGLM (Ours)	45.4	47.2	44.3	45.7

Table 6. Comparison (%) on VSGR for the Video Captioning.

Method	CIDEr	MENTOR	ROUGE-L	BLEU-4
MV-GPT [38]	57.1	37.5	62.5	47.2
CoCap [40]	54.3	29.4	61.8	42.8
UniVL + MELTR [24]	50.5	28.1	60.0	42.1
HyperGLM (Ours)	54.5	30.7	64.9	48.8

capture the temporal evolution of relationships by modeling sequential interactions and their dependencies. In contrast, NeuralODE and NeuralSDE primarily focus on continuous-time dynamics, which may limit their effectiveness in handling discrete, multi-step relational changes as illustrated in Fig. 7b. Significantly, the HyperGraph is injected into the LLM, allowing the model to capture complex temporal patterns, resulting in better results than the HyperGraph.

In addition to the improvements in SGG and SGA shown in Fig. 7, Tables 5, 6, and 7 demonstrate the significant improvements using our HyperGLM approach in the VQA, VC, and RR tasks. In VQA, the hyperedges connect multiple objects, enabling HyperGLM to capture context-rich interactions more effectively, reaching an accuracy of 45.4%. For VC, the HyperGraph structure supports evolving object connections over time, allowing our HyperGLM approach to generate captions that describe the relationship between objects and capture the temporal flow of interactions coher-

Table 7. Comparison (%) on VSGR for the Relation Reasoning.

Method	Accuracy	Precision	Recall	F1 Score
Video-LLaVA-7B [30]	41.3	42.5	40.2	41.3
MA-LMM [14]	42.8	43.7	41.8	42.7
LLaMA-VID-7B [29]	44.1	45.2	43.5	44.3
HyperGLM (Ours)	47.2	48.4	46.5	47.4

ently, achieving scores of 54.5% at CIDEr and 64.9% at ROUGE-L. In RR task, the HyperGraph effectively manages intricate dependencies between multiple objects, resulting in precise relational inferences with an accuracy of 47.2%.

7. Conclusion

In this paper, we have introduced HyperGLM, a novel VidSGG method that integrates scene hypergraph information into LLMs for context-aware and precise scene interpretation. Our approach effectively models complex interactions and higher-order relationships. It outperforms leading methods on benchmarks, including PVSG, Action Genome, and our newly collected VSGR dataset across five tasks.

Limitations. Although our HyperGLM approach effectively models multi-way interactions, managing many objects and their interactions can complicate relationship structures. As the HyperGraph expands, essential relationships may become obscured, reducing the clarity of scene interpretation.

Acknowledgment. This material is based upon work supported by the National Science Foundation under Award No. OIA-1946391. We also acknowledge the Arkansas High-Performance Computing Center for providing GPUs.

References

- [1] Song Bai, Feihu Zhang, and Philip HS Torr. Hypergraph convolution and hypergraph attention. *Pattern Recognition*, 110:107637, 2021. [2](#)
- [2] Joya Chen, Zhaoyang Lv, Shiwei Wu, Kevin Qinghong Lin, Chenan Song, Difei Gao, Jia-Wei Liu, Ziteng Gao, Dongxing Mao, and Mike Zheng Shou. Videollm-online: Online video large language model for streaming video. In *Proceedings of the IEEE/CVF Conference on Computer Vision and Pattern Recognition*, pages 18407–18418, 2024. [1](#)
- [3] Zhanwen Chen, Saeid Rezayi, and Sheng Li. More knowledge, less bias: Unbiasing scene graph generation with explicit ontological adjustment. In *Proceedings of the IEEE/CVF Winter Conference on Applications of Computer Vision*, pages 4023–4032, 2023. [2](#)
- [4] Yuren Cong, Wentong Liao, Hanno Ackermann, Bodo Rosenhahn, and Michael Ying Yang. Spatial-temporal transformer for dynamic scene graph generation. In *Proceedings of the IEEE/CVF international conference on computer vision*, pages 16372–16382, 2021. [1, 2, 3](#)
- [5] Yuren Cong, Wentong Liao, H. Ackermann, M. Yang, and B. Rosenhahn. Spatial-temporal transformer for dynamic scene graph generation. *IEEE International Conference on Computer Vision*, 2021. [7](#)
- [6] Yuren Cong, Michael Ying Yang, and Bodo Rosenhahn. Reltr: Relation transformer for scene graph generation. *IEEE Transactions on Pattern Analysis and Machine Intelligence*, 45(9):11169–11183, 2023. [2](#)
- [7] Youming Deng, Yansheng Li, Yongjun Zhang, Xiang Xiang, Jian Wang, Jingdong Chen, and Jiayi Ma. Hierarchical memory learning for fine-grained scene graph generation. In *European Conference on Computer Vision*, pages 266–283. Springer, 2022. [2](#)
- [8] Alexey Dosovitskiy, Lucas Beyer, Alexander Kolesnikov, Dirk Weissenborn, Xiaohua Zhai, Thomas Unterthiner, Mostafa Dehghani, Matthias Minderer, Georg Heigold, Sylvain Gelly, Jakob Uszkoreit, and Neil Houlsby. An image is worth 16x16 words: Transformers for image recognition at scale. In *International Conference on Learning Representations*, 2021. [6](#)
- [9] Azade Farshad, Yousef Yeganeh, Yu Chi, Chengzhi Shen, Böjrn Ommer, and Nassir Navab. Scenegenie: Scene graph guided diffusion models for image synthesis. In *Proceedings of the IEEE/CVF International Conference on Computer Vision*, pages 88–98, 2023. [2](#)
- [10] Hao Fei, Shengqiong Wu, Wei Ji, Hanwang Zhang, Meishan Zhang, Mong-Li Lee, and Wynne Hsu. Video-of-thought: Step-by-step video reasoning from perception to cognition. In *Forty-first International Conference on Machine Learning*, 2024. [1](#)
- [11] Shengyu Feng, Hesham Mostafa, Marcel Nassar, Somdeb Majumdar, and Subarna Tripathi. Exploiting long-term dependencies for generating dynamic scene graphs. *IEEE Workshop/Winter Conference on Applications of Computer Vision*, 2021. [7](#)
- [12] Yue Gao, Yifan Feng, Shuyi Ji, and Rongrong Ji. Hgnn+: General hypergraph neural networks. *IEEE Transactions on Pattern Analysis and Machine Intelligence*, 45(3):3181–3199, 2022. [2](#)
- [13] Zeeshan Hayder and Xuming He. Dsgg: Dense relation transformer for an end-to-end scene graph generation. In *Proceedings of the IEEE/CVF Conference on Computer Vision and Pattern Recognition*, pages 28317–28326, 2024. [2](#)
- [14] Bo He, Hengduo Li, Young Kyun Jang, Menglin Jia, Xuefei Cao, Ashish Shah, Abhinav Shrivastava, and Ser-Nam Lim. Ma-lmm: Memory-augmented large multimodal model for long-term video understanding. In *Proceedings of the IEEE/CVF Conference on Computer Vision and Pattern Recognition*, pages 13504–13514, 2024. [8](#)
- [15] Tao He, Lianli Gao, Jingkuan Song, and Yuan-Fang Li. Towards open-vocabulary scene graph generation with prompt-based finetuning. In *European Conference on Computer Vision*, pages 56–73. Springer, 2022. [2](#)
- [16] Edward J Hu, yelong shen, Phillip Wallis, Zeyuan Allen-Zhu, Yuanzhi Li, Shean Wang, Lu Wang, and Weizhu Chen. LoRA: Low-rank adaptation of large language models. In *International Conference on Learning Representations*, 2022. [6](#)
- [17] Jinbae Im, JeongYeon Nam, Nokyung Park, Hyungmin Lee, and Seunghyun Park. Egrt: Extracting graph from transformer for scene graph generation. In *Proceedings of the IEEE/CVF Conference on Computer Vision and Pattern Recognition*, pages 24229–24238, 2024. [2](#)
- [18] Jingwei Ji, Ranjay Krishna, Li Fei-Fei, and Juan Carlos Niebles. Action genome: Actions as compositions of spatio-temporal scene graphs. In *Proceedings of the IEEE/CVF Conference on Computer Vision and Pattern Recognition*, pages 10236–10247, 2020. [1, 2, 5, 6, 7](#)
- [19] Albert Q Jiang, Alexandre Sablayrolles, Arthur Mensch, Chris Bamford, Devendra Singh Chaplot, Diego de las Casas, Florian Bressand, Gianna Lengyel, Guillaume Lampe, Lucile Saulnier, et al. Mistral 7b. *arXiv preprint arXiv:2310.06825*, 2023. [6](#)
- [20] Peng Jin, Ryuichi Takanobu, Wancai Zhang, Xiaochun Cao, and Li Yuan. Chat-univi: Unified visual representation empowers large language models with image and video understanding. In *Proceedings of the IEEE/CVF Conference on Computer Vision and Pattern Recognition*, pages 13700–13710, 2024. [1, 8](#)
- [21] Tianlei Jin, Fangtai Guo, Qiwei Meng, Shiqiang Zhu, Xiangming Xi, Wen Wang, Zonghao Mu, and Wei Song. Fast contextual scene graph generation with unbiased context augmentation. In *Proceedings of the IEEE/CVF Conference on Computer Vision and Pattern Recognition*, pages 6302–6311, 2023. [2](#)
- [22] Eun-Sol Kim, Woo Young Kang, Kyoung-Woon On, Yu-Jung Heo, and Byoung-Tak Zhang. Hypergraph attention networks for multimodal learning. In *Proceedings of the IEEE/CVF conference on computer vision and pattern recognition*, pages 14581–14590, 2020. [2](#)
- [23] Kibum Kim, Kanghoon Yoon, Jaehyeong Jeon, Yeonjun In, Jinyoung Moon, Donghyun Kim, and Chanyoung Park. Llm4sgg: Large language models for weakly supervised scene graph generation. In *Proceedings of the IEEE/CVF Conference on Computer Vision and Pattern Recognition*, pages 28306–28316, 2024. [2](#)
- [24] Dohwan Ko, Joonmyung Choi, Hyeong Kyu Choi, Kyoung-

- Woon On, Byungseok Roh, and Hyunwoo J Kim. Meltr: Meta loss transformer for learning to fine-tune video foundation models. In *Proceedings of the IEEE/CVF Conference on Computer Vision and Pattern Recognition*, pages 20105–20115, 2023. 1, 8
- [25] Sanjoy Kundu and Sathyaranayanan N Aakur. Is-ggt: Iterative scene graph generation with generative transformers. In *Proceedings of the IEEE/CVF Conference on Computer Vision and Pattern Recognition*, pages 6292–6301, 2023. 2
- [26] Rongjie Li, Songyang Zhang, and Xuming He. Sgtr: End-to-end scene graph generation with transformer. In *proceedings of the IEEE/CVF conference on computer vision and pattern recognition*, pages 19486–19496, 2022. 2
- [27] Rongjie Li, Songyang Zhang, Dahua Lin, Kai Chen, and Xuming He. From pixels to graphs: Open-vocabulary scene graph generation with vision-language models. In *Proceedings of the IEEE/CVF Conference on Computer Vision and Pattern Recognition*, pages 28076–28086, 2024. 2
- [28] Wanxin Li, Wei Xie, Zhigang Tu, Wei Wang, and Lianghai Jin. Multi-hyperedge hypergraph for group activity recognition. In *2022 International Joint Conference on Neural Networks (IJCNN)*, pages 01–07. IEEE, 2022. 2
- [29] Yanwei Li, Chengyao Wang, and Jiaya Jia. Llama-vid: An image is worth 2 tokens in large language models. In *European Conference on Computer Vision*, pages 323–340. Springer, 2025. 8
- [30] Bin Lin, Yang Ye, Bin Zhu, Jiaxi Cui, Munan Ning, Peng Jin, and Li Yuan. Video-llava: Learning united visual representation by alignment before projection. *arXiv preprint arXiv:2311.10122*, 2023. 1, 8
- [31] Haotian Liu, Chunyuan Li, Qingyang Wu, and Yong Jae Lee. Visual instruction tuning. *Advances in neural information processing systems*, 36, 2024. 6
- [32] Muhammad Maaz, Hanoona Rasheed, Salman Khan, and Fahad Khan. Video-ChatGPT: Towards detailed video understanding via large vision and language models. In Lun-Wei Ku, Andre Martins, and Vivek Srikanth, editors, *Proceedings of the 62nd Annual Meeting of the Association for Computational Linguistics (Volume 1: Long Papers)*, pages 12585–12602, Bangkok, Thailand, Aug. 2024. Association for Computational Linguistics. 1, 8
- [33] Sayak Nag, Kyle Min, Subarna Tripathi, and Amit K Roy-Chowdhury. Unbiased scene graph generation in videos. In *Proceedings of the IEEE/CVF Conference on Computer Vision and Pattern Recognition*, pages 22803–22813, 2023. 2
- [34] Trong-Thuan Nguyen, Pha Nguyen, and Khoa Luu. Hig: Hierarchical interlacement graph approach to scene graph generation in video understanding. In *Proceedings of the IEEE/CVF Conference on Computer Vision and Pattern Recognition*, 2024. 1, 2, 3, 5, 7
- [35] Trong-Thuan Nguyen, Pha Nguyen, Li Xin, Cothren Jackson, Yilmaz Alper, and Khoa Luu. CYCLO: Cyclic graph transformer approach to multi-object relationship modeling in aerial videos. In *The Thirty-eighth Annual Conference on Neural Information Processing Systems*, 2024. 1, 2, 5, 7
- [36] Rohith Peddi, Saksham Singh, Parag Singla, Vibhav Gogate, et al. Towards scene graph anticipation. In *European Conference on Computer Vision*. Springer, 2024. 1, 2, 3, 7, 8
- [37] Alec Radford, Jong Wook Kim, Chris Hallacy, Aditya Ramesh, Gabriel Goh, Sandhini Agarwal, Girish Sastry, Amanda Askell, Pamela Mishkin, Jack Clark, et al. Learning transferable visual models from natural language supervision. In *International conference on machine learning*, pages 8748–8763. PMLR, 2021. 6
- [38] Paul Hongsoon Seo, Arsha Nagrani, Anurag Arnab, and Cordelia Schmid. End-to-end generative pretraining for multimodal video captioning. In *Proceedings of the IEEE/CVF Conference on Computer Vision and Pattern Recognition*, pages 17959–17968, 2022. 1, 8
- [39] Xindi Shang, Yicong Li, Junbin Xiao, Wei Ji, and Tat-Seng Chua. Video visual relation detection via iterative inference. In *Proceedings of the 29th ACM international conference on Multimedia*, pages 3654–3663, 2021. 2
- [40] Yaojie Shen, Xin Gu, Kai Xu, Heng Fan, Longyin Wen, and Libo Zhang. Accurate and fast compressed video captioning. In *Proceedings of the IEEE/CVF International Conference on Computer Vision*, pages 15558–15567, 2023. 1, 8
- [41] Enxin Song, Wenhao Chai, Guanhong Wang, Yucheng Zhang, Haoyang Zhou, Feiyang Wu, Haozhe Chi, Xun Guo, Tian Ye, Yanting Zhang, et al. Moviechat: From dense token to sparse memory for long video understanding. In *Proceedings of the IEEE/CVF Conference on Computer Vision and Pattern Recognition*, pages 18221–18232, 2024. 1, 8
- [42] Yao Teng, Limin Wang, Zhifeng Li, and Gangshan Wu. Target adaptive context aggregation for video scene graph generation. In *Proceedings of the IEEE/CVF International Conference on Computer Vision*, pages 13688–13697, 2021. 1, 2, 3
- [43] Nupur Thakur, PrasanthSai Gouripeddi, and Baoxin Li. Graph (graph): A nested graph-based framework for early accident anticipation. In *Proceedings of the IEEE/CVF Winter Conference on Applications of Computer Vision*, pages 7533–7541, 2024. 1, 2
- [44] Aisha Urooj, Hilde Kuehne, Bo Wu, Kim Chheu, Walid Boushelham, Chuang Gan, Niels Lobo, and Mubarak Shah. Learning situation hyper-graphs for video question answering. In *Proceedings of the IEEE/CVF Conference on Computer Vision and Pattern Recognition*, pages 14879–14889, 2023. 2
- [45] Jiahao Wang, Guo Chen, Yifei Huang, Limin Wang, and Tong Lu. Memory-and-anticipation transformer for online action understanding. In *Proceedings of the IEEE/CVF International Conference on Computer Vision*, pages 13824–13835, 2023. 1
- [46] Yanan Wang, Shuichiro Haruta, Donghuo Zeng, Julio Vizcarra, and Mori Kurokawa. Multi-object event graph representation learning for video question answering. In *Meeting on Image Recognition and Understanding*, 2024. 2
- [47] Tao Wu, Runyu He, Gangshan Wu, and Limin Wang. Sportshhi: A dataset for human-human interaction detection in sports videos. In *Proceedings of the IEEE/CVF Conference on Computer Vision and Pattern Recognition*, 2024. 2, 5
- [48] Dejing Xu, Zhou Zhao, Jun Xiao, Fei Wu, Hanwang Zhang, Xiangnan He, and Yueting Zhuang. Video question answering via gradually refined attention over appearance and motion. In *Proceedings of the 25th ACM international conference on Multimedia*, pages 1645–1653, 2017. 6
- [49] Jun Xu, Tao Mei, Ting Yao, and Yong Rui. Msr-vtt: A large video description dataset for bridging video and language. In *Proceedings of the IEEE conference on computer vision and*

- pattern recognition*, pages 5288–5296, 2016. 6
- [50] Zenan Xu, Wanjun Zhong, Qinliang Su, Zijing Ou, and Fuwei Zhang. Modeling semantic composition with syntactic hypergraph for video question answering. *arXiv preprint arXiv:2205.06530*, 2022. 2
- [51] Jingkang Yang, Yi Zhe Ang, Zujin Guo, Kaiyang Zhou, Wayne Zhang, and Ziwei Liu. Panoptic scene graph generation. In *European Conference on Computer Vision*, pages 178–196. Springer, 2022. 2
- [52] Jingkang Yang, Wenxuan Peng, Xiangtai Li, Zujin Guo, Liangyu Chen, Bo Li, Zheng Ma, Kaiyang Zhou, Wayne Zhang, Chen Change Loy, et al. Panoptic video scene graph generation. In *Proceedings of the IEEE/CVF Conference on Computer Vision and Pattern Recognition*, pages 18675–18685, 2023. 1, 2, 5, 6, 7
- [53] Guangyao Zhai, Evin Pınar Örnek, Shun-Cheng Wu, Yan Di, Federico Tombari, Nassir Navab, and Benjamin Busam. Commonsenes: Generating commonsense 3d indoor scenes with scene graphs. *Advances in Neural Information Processing Systems*, 36, 2024. 2
- [54] Zizhao Zhang, Yifan Feng, Shihui Ying, and Yue Gao. Deep hypergraph structure learning. *arXiv preprint arXiv:2208.12547*, 2022. 2
- [55] Xiaolin Zhu, Dongli Wang, Jianxun Li, Rui Su, Qin Wan, and Yan Zhou. Dynamical attention hypergraph convolutional network for group activity recognition. *IEEE Transactions on Neural Networks and Learning Systems*, 2024. 2